

# High-Order, Conservative Discontinuous Galerkin Algorithms for (Gyro) Kinetic Simulations of Edge Plasma

A. H. Hakim   G. W. Hammett

Princeton Plasma Physics Laboratory, Princeton, NJ  
ammar@princeton.edu  
<http://www.ammar-hakim.org>

American Physical Society, Division of Plasma Physics,  
29<sup>th</sup> October- 2<sup>nd</sup> November 2012

## Long term goal: Accurate and stable continuum schemes for full-F edge gyrokinetics in 3D geometries

Question: Can one develop accurate and stable schemes that conserve invariants, maintain positivity and use as few grid points as possible?

### Proposed Answer

Explore high-order hybrid discontinuous/continuous Galerkin finite-element schemes, enhanced with flux-reconstruction and a proper choice of velocity space basis functions.

## Several fluid and kinetic problems are described by a Hamiltonian

$$\frac{\partial f}{\partial t} = \{H, f\}$$

where  $H(z^1, z^2)$  is the Hamiltonian and canonical Poisson bracket is

$$\{g, h\} \equiv \frac{\partial g}{\partial z^1} \frac{\partial h}{\partial z^2} - \frac{\partial g}{\partial z^2} \frac{\partial h}{\partial z^1}.$$

Defining phase-space velocity vector  $\alpha = (\dot{z}^1, \dot{z}^2)$ , with  $\dot{z}^i = \{z^i, H\}$  leads to *phase-space conservation form*

$$\frac{\partial f}{\partial t} + \nabla \cdot (\alpha f) = 0.$$

Additionally  $\nabla \cdot \alpha = 0$  (Liouville theorem).

## Example: Incompressible Euler equations in two dimensions serves as a model for $E \times B$ nonlinearities in gyrokinetics

A basic model problem is the *incompressible* 2D Euler equations written in the stream-function ( $\phi$ ) vorticity ( $f$ ) formulation. Here the Hamiltonian is simply  $H(x, y) = \phi(x, y)$ .

$$\frac{\partial f}{\partial t} + \nabla \cdot (\mathbf{u}f) = 0$$

where  $u_x = \{x, H\} = \partial\phi/\partial y$  and  $u_y = \{y, H\} = -\partial\phi/\partial x$ . The potential is determined from

$$\nabla^2\phi = -f.$$

## Example: Vlasov equation for electrostatic plasmas

The Vlasov-Poisson system has the Hamiltonian

$$H(x, p) = \frac{1}{2m}p^2 + q\phi(x)$$

where  $q$  is species charge and  $m$  is species mass and  $p = mv$  is momentum. With this  $\dot{x} = v$  and  $\dot{v} = -q\partial\phi/\partial x$  leading to

$$\frac{\partial f}{\partial t} + v \frac{\partial f}{\partial x} - \frac{q}{m} \frac{\partial \phi}{\partial x} \frac{\partial f}{\partial v} = 0$$

## For Vlasov equation potential can be determined in two different ways

For electron plasma waves use full Poisson equation

$$\frac{\partial^2 \phi}{\partial x^2} = -\frac{\rho_c}{\epsilon_0}$$

where  $\rho_c = |e|(n_{io}(x) - n(x, t))$  is total charge density. For ion-acoustic waves use quasi-neutrality

$$n_i(x) = n_{eo} \left( 1 + \frac{|e|\phi}{T_e} \right)$$

where  $n_{eo}$  is the constant electron initial density and  $T_e$  is the fixed electron temperature. This determines potential without the need to solve a Poisson equation and is a model of parallel dynamics in gyrokinetics.

## Gyrokinetic equation can also be derived from gyro-center Hamiltonian

In the Hamiltonian gyrokinetic theory<sup>1</sup> the gyrokinetic equation is derived from the gyrocentre Hamiltonian in gyro-center coordinates  $(\mathbf{R}, v_{\parallel}, \mu, \alpha)$

$$H = \frac{1}{2} m_i v_{\parallel}^2 + \mu B + e_i \langle \phi \rangle_{\alpha}$$

where  $v_{\parallel}$  is the parallel velocity,  $\mu$  is the magnetic moment,  $\alpha$  is gyro-angle and  $\phi$  is the electrostatic potential. Poisson bracket is no longer canonical, but gyrokinetic Vlasov equation can still be written as a conservation equation in phase-space.

---

<sup>1</sup>A Brizard and T Hahm. "Foundations of nonlinear gyrokinetic theory". In: *Reviews of Modern Physics* 79.2 (Apr. 2007), pp. 421–468.

## Invariants for Hamiltonian systems can be derived by looking at *weak-form* of equations

Multiplying conservation law form by a smooth test function  $w(x, v)$  and integrating over an arbitrary volume element  $K$  gives the weak-form

$$\int_K w \frac{\partial f}{\partial t} d\Omega + \int_{\partial K} w^- \alpha \cdot \mathbf{n} f dS - \int_K \nabla w \cdot \alpha f d\Omega = 0.$$

Picking  $w = 1$  leads to (with periodic boundary conditions) *particle conservation*

$$\frac{d}{dt} \int_K f d\Omega = 0.$$

## Energy conservation is derived using Hamiltonian itself as test function

Substituting the Hamiltonian for the test function and using the identity  $\nabla H \cdot \alpha = 0$  leads to

$$\int_{\mathcal{K}} H \frac{\partial f}{\partial t} d\Omega = 0.$$

For the incompressible Euler equation this becomes

$$\frac{\partial}{\partial t} \int_{\mathcal{K}} \frac{1}{2} |\nabla \phi|^2 d\Omega = 0.$$

For the Vlasov-Poisson system this becomes

$$\frac{\partial}{\partial t} \int \mathcal{E} + \frac{\epsilon_0}{2} \left( \frac{\partial \phi}{\partial x} \right)^2 dx = 0$$

where  $\mathcal{E}(x, t) \equiv \frac{1}{2} \int_{-\infty}^{\infty} mv^2 f dv$  is the fluid energy.

## Generalized entropy (enstrophy) conservation can be derived using the solution as test function

The solution itself can be used as a test function. This gives

$$\int_{\mathcal{K}} f \frac{\partial f}{\partial t} d\Omega + \int_{\partial\mathcal{K}} f^{-} \boldsymbol{\alpha} \cdot \mathbf{n} f dS - \int_{\mathcal{K}} \nabla f \cdot \boldsymbol{\alpha} f d\Omega = 0.$$

As  $\nabla f \cdot \boldsymbol{\alpha} f = \nabla \cdot (\boldsymbol{\alpha} f^2/2)$  the last term reduces to a surface integral, leading to

$$\frac{\partial}{\partial t} \int_{\mathcal{K}} \frac{1}{2} f^2 d\Omega = 0.$$

## Vlasov-Poisson system also admits momentum conservation

For the Vlasov-Poisson system we can select the coordinate  $v$  as the test function. This leads to

$$\int_K v \frac{\partial f}{\partial t} d\Omega + \int_{\partial K} v \alpha \cdot \mathbf{n} f dS - \int_K \nabla v \cdot \alpha f d\Omega = 0.$$

As  $\nabla v \cdot \alpha = \{v, H\} = \dot{v}f$  the last term becomes

$$\int_K \dot{v} f d\Omega = \int \frac{|e|}{m} \frac{\partial \phi}{\partial x} n dx.$$

Using the Poisson equation to eliminate  $n(x, t)$ , integrating by parts and applying boundary condition leads to the momentum conservation law

$$\frac{d}{dt} \int_K v f d\Omega = 0.$$

## A discontinuous finite element scheme is used to discretize Hamiltonian equation

To discretize the equations introduce a triangulation  $K_\nu$  of the domain  $K$ . Pick a finite-dimensional function space

$$\mathcal{V}_m^k(K) \equiv \{w : w|_{K_\nu} \in P^k(K_\nu)\} \cap C^m$$

where  $P^k(K_\nu)$  is the space of polynomials of order at most  $k$  on the element  $K_\nu$ . Then the discrete problem is stated as: find  $f_h \in \mathcal{V}_{-1}^k$  such that for all smooth  $w$  we have

$$\int_{K_\nu} w \frac{\partial f_h}{\partial t} d\Omega + \int_{\partial K_\nu} w^- \mathbf{n} \cdot \alpha_h \hat{f}_h dS - \int_{K_\nu} \nabla w \cdot \alpha_h f_h d\Omega = 0.$$

Here  $\hat{f}_h = \hat{f}(f_h^+, f_h^-)$  is the consistent *numerical flux* on  $\partial K_\nu$ .

## A continuous finite element scheme is used to discretize Poisson equation

To discretize the Poisson equation the problem is stated as: find  $\phi_h \in \mathcal{V}_0^r$  such that for all smooth  $\psi$  we have

$$\int_K \psi \nabla^2 \phi_h d\Omega = \int_K \psi s d\Omega$$

where  $s$  represents the sources. For ion-acoustic waves the number density and potential are related by a *projection* operator: find  $\phi_h \in \mathcal{V}_0^k$  given a  $n_{ih} \in \mathcal{V}_{-1}^k$  such that for all smooth  $w$

$$\int w n_{ih} dx = n_{eo} \int w \left( 1 + \frac{|e| \phi_h}{T_e} \right) dx$$

This leads to a *global* solve for the potential. For the case in which potential is allowed to be *discontinuous* leading hence a local determination of the potential, see poster by G. Hammett.

## Only recently conditions for conservation of discrete energy and enstrophy were discovered

Liu and Shu<sup>2</sup> have shown that discrete energy is conserved for 2D incompressible flow if

$$\phi_h \in \mathcal{V}_0^k \subseteq f_h \in \mathcal{V}_{-1}^k$$

Enstrophy (generalized entropy) is conserved if *central fluxes* are used in the DG scheme. With upwind fluxes, enstrophy decays and hence the scheme is *stable* in the  $L_2$  norm.

---

<sup>2</sup>J-G Liu and C-W Shu. "A High Order Discontinuous Galerkin Method for 2D Incompressible Flows". In: *Journal of Computational Physics* (2000).

## Momentum conservation is not exact but is independent of velocity resolution

For electrostatic problems the condition for conservation of discrete momentum reduces to a vanishing average force, i.e. we must have

$$\int n_h E_h dx = 0$$

However, one can show that as  $E_h$  is discontinuous, the present scheme *does not* satisfy this condition, and hence momentum is not conserved.

One can imagine that projecting  $E_h \in \mathcal{V}_{-1}^{k-1}$  to a smoother space  $\mathcal{V}_0^{k-1}$  to make it continuous would help. However, even with a projection momentum is not conserved. Solving the Poisson equation with higher order continuity ( $\phi_h \in \mathcal{V}_1^r$ ) also does not help as then the energy conservation condition is violated.

## Prototype code named Gkeyll has been developed

- ▶ Gkeyll is written in C++ and is inspired by framework efforts like Facets, VORPAL (Tech-X Corporation) and WarpX (U. Washington). Uses structured grids with arbitrary dimension/order nodal basis functions.
- ▶ Linear solvers from Petsc<sup>3</sup> are used for inverting stiffness matrices.
- ▶ Games programming language Lua<sup>4</sup>, used in games like World of Warcraft (10 million users), is used as an embedded scripting language to drive simulations.
- ▶ MPI is used for parallelization via the txbase library developed at Tech-X Corporation.
- ▶ Package management and builds are automated via scimake and bilder, both developed at Tech-X Corporation.

---

<sup>3</sup><http://www.mcs.anl.gov/petsc/>

<sup>4</sup><http://www.lua.org>

A simulation journal with results is maintained at <http://www.ammar-hakim.org/sj>

- ▶ Each algorithm is carefully tested against analytical or numerical results.
- ▶ Results are extensively documented and Lua programs are put online.
- ▶ Journal allows sharing of results as well as enables reproducibility as scripts, figures and notes are available via the internet.

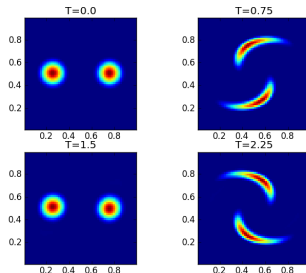


Figure: Swirling flow problem. The initial Gaussian pulses distort strongly but regain their shapes after a period of 1.5 seconds.

# Accuracy and convergence of schemes was tested with Vlasov equation with specified potential: $\cos(x)$ potential well

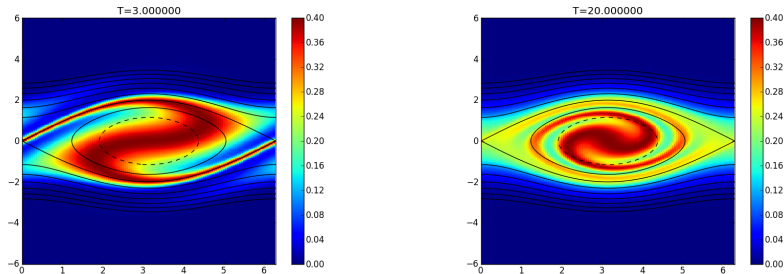


Figure: Distribution function at  $t = 3$  (left) and  $t = 20$  (right) for flow in a  $\cos(x)$  potential well. A separatrix forms along the trapped-passing boundary. Simulation run with a DG2 scheme on a  $64 \times 128$  grid.

With quadratic potential  $\phi(x) = x^2$  a rigid-body motion of trapped particles in phase-space is seen

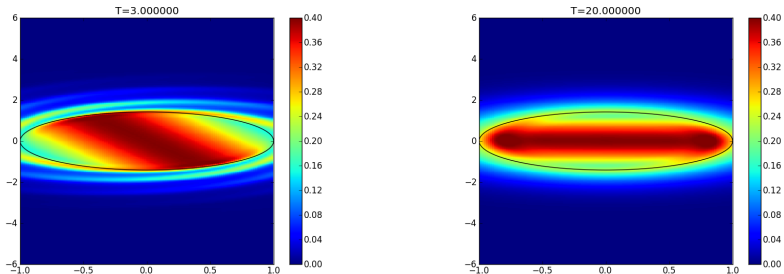
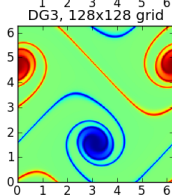
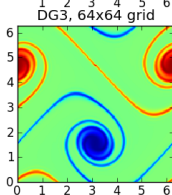
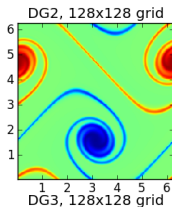
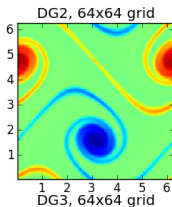


Figure: Distribution function at  $t = 3$  (left) and  $t = 20$  (right) for flow in a  $x^2$  potential well. Bounce period of all trapped particles is the same, leading to a rigid-body motion inside trapped region.

# Double shear problem is a good test for resolution of vortex shearing in $E \times B$ driven flows

Vorticity at  $t = 8$  with different grid resolutions and schemes. Third order DG scheme runs faster and produces better results than DG2 scheme.



# Vortex waltz problem tests resolution of small-scale vortex features and energy and enstrophy conservation

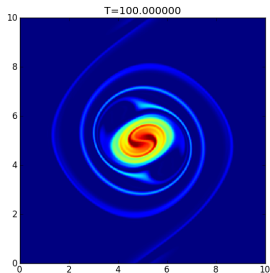


Figure: Vorticity for the vortex waltz problem with the third-order scheme on a  $128 \times 128$ . *Upwind fluxes* were used for this calculation.

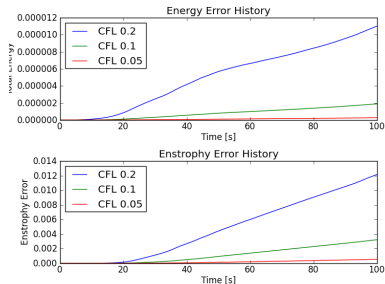
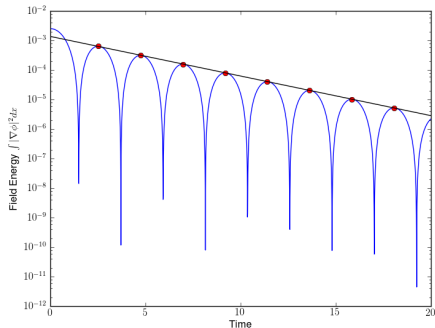


Figure: Energy and enstrophy error for vortex waltz problem. *Central fluxes* were used and show  $O(\Delta t)^3$  convergence on a fixed  $64 \times 64$  grid.

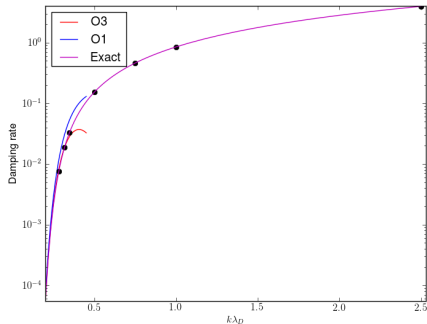
## Linear Landau damping simulations were compared with exact solutions of dispersion relations

Field energy (blue) as a function of time for linear Landau damping problem with  $k = 0.5$  and  $Te = 1.0$ . The red dots represent the maxima in the field energy which are used to compute a linear least-square fit. The slope of the black line gives the damping rate.



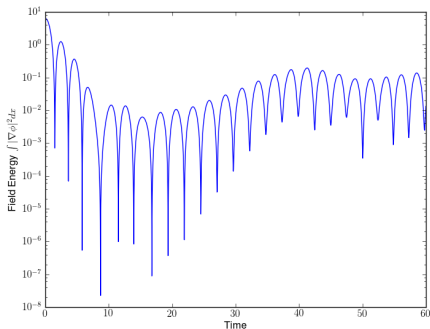
# Numerically computed damping rates compare accurately with exact results

Damping rate from Landau damping for electron plasma oscillations as a function of normalized Debye length. The damping rates are within 3% of the exact values, and for large values of  $k\lambda_D$  within 1%.

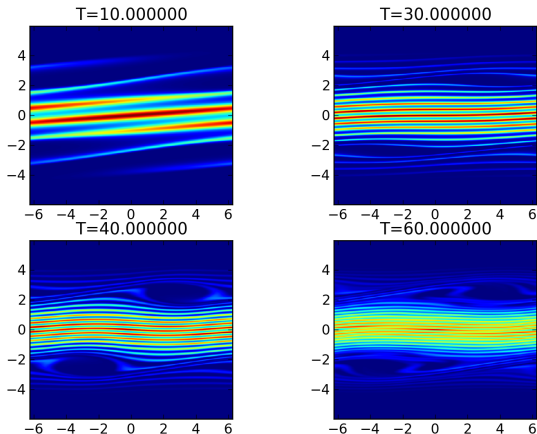


# Nonlinear Landau damping simulations show particle trapping and phase-space hole formation

Field energy as a function of time for nonlinear Landau damping problem with  $k=0.5$ ,  $T_e = 1.0$  and  $\alpha = 0.5$ . The initial perturbation decays at a rate of  $\gamma = 0.2916$ , after which the damping is halted from particle trapping. The growth rate of this phase is  $\gamma = 0.0879$ .



# DG scheme can efficiently capture fine-scale features in phase-space



Energy is conserved to same order as temporal discretization error of  $O(\Delta t)^3$  independent of phase-space discretization

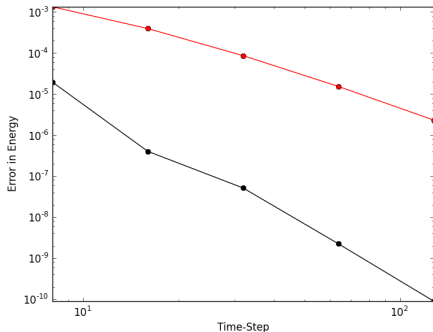


Figure: Convergence of energy error with time-step. The red curve shows errors from second order scheme, black from third order scheme.

To test momentum conservation an asymmetric initial density profile needs to be used

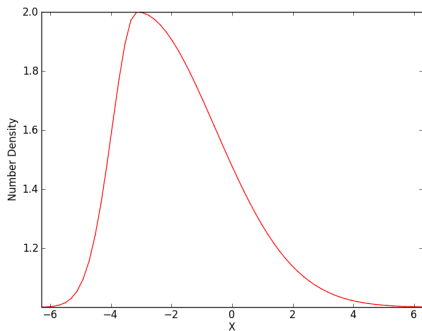


Figure: Initial density profile to drive momentum. Using a symmetric density (net zero initial momentum) profile can lead to misleading conservation results.

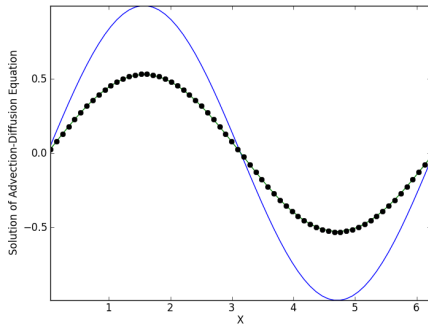
Momentum is *not conserved* but is independent of velocity space resolution and converges rapidly with spatial resolution and polynomial order

$N_x$	Error DG2	Order
8	$1.3332 \times 10^{-3}$	
16	$3.9308 \times 10^{-4}$	1.76
32	$8.5969 \times 10^{-5}$	2.19
64	$1.5254 \times 10^{-5}$	2.49
128	$2.3105 \times 10^{-6}$	2.72

$N_x$	Error DG3	Order
8	$1.9399 \times 10^{-5}$	
16	$4.0001 \times 10^{-7}$	5.60
32	$5.1175 \times 10^{-8}$	2.97
64	$2.2289 \times 10^{-9}$	4.52
128	$8.9154 \times 10^{-11}$	4.64

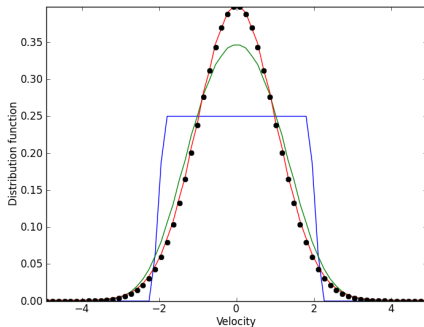
## A local-DG scheme is used to discretize diffusion terms for use in collision operators

Advection-diffusion problem with local DG scheme. The initial condition is  $\sin(x)$  for which the exact solution at time  $t$  is  $e^{-\alpha t} \sin(x - \lambda t)$  where  $\alpha$  is the diffusion coefficient and  $\lambda$  is advection velocity. Black dots are exact solutions and solid lines numerical results.



# A particle, momentum and energy conserving Lenard-Bernstein collision operator is implemented using local DG diffusion solver

Relaxation of a  
step-function distribution  
function to Maxwellian  
due to collisions. The solid  
lines show distribution  
function at different times  
and the dots the exact  
Maxwellian distribution  
with specified temperature  
and density.



## Conclusions: An efficient and accurate discontinuous Galerkin scheme for general Hamiltonian field equations is presented

- ▶ A discontinuous Galerkin scheme to solve a general class of Hamiltonian field equations is presented.
- ▶ The Poisson equation is discretized using continuous basis functions.
- ▶ With proper choice of basis functions energy is conserved.
- ▶ With central fluxes enstrophy (generalize entropy) is conserved. With upwind fluxes the scheme is  $L_2$  stable.
- ▶ Momentum is not conserved but is independent of velocity space resolution and converges rapidly with spatial resolution and polynomial order of the scheme.

## Future work: extend scheme to higher dimensions and general geometries and collision terms

- ▶ Higher-order basis functions have been implemented and are being tested.
- ▶ The schemes will be extended to take into account complicated edge geometries using a multi-block structured grid.
- ▶ Special basis functions for velocity space discretization will be developed to allow coarse resolution simulations with the option of fine scale resolution when needed.
- ▶ A collision model has been implemented. It will be extended to higher dimensions.